



Characterization of Granular Materials Treated with Fly Ash for Road Infrastructure Applications

Hamou Azaiez^{1,2} · Abdellah Cherif Taiba² · Youcef Mahmoudi² · Mostefa Belkhatir^{2,3}

Accepted: 3 August 2020 / Published online: 13 August 2020
© Springer Science+Business Media, LLC, part of Springer Nature 2020

Abstract

This paper presents the results of an experimental investigation carried out to evaluate the effects of fly ash (FA) on the coarse-grained soils compaction response and shear characteristics for the purpose to valorize their utilization as local materials in road infrastructure applications. A series of compaction and direct shear tests was performed on three different classes derived from natural Chlef sand having different maximum grain sizes mixed with fly ash according to percentages ranging from 0% to 15%. The sand-fly ash mixture samples were reconstituted with water content varying between 4% and 14% for the whole experimental compaction testing program. The obtained data confirmed that the particle size and fly ash content have a significant influence on the mechanical performance (in terms of compaction response and shear strength characteristics) of sand-fly ash mixtures. Indeed, the increase of the maximum particle size and fly ash fraction induced a noticeable increase of the maximum dry density and decrease of the optimum water content for the tested sand-fly ash mixture samples. On the other hand, the obtained test results indicated clearly the impact of D_{\max} and FA on the shear strength response of the sand-fly ash mixtures for the fly ash content range (0%–15%) under study. The newly introduced particle size characteristics appeared as pertinent parameters to predict the compaction response and shear strength characteristics of the tested materials.

Keywords Compaction · Shear strength characteristics · Particle size · Sand-fly ash mixtures · Road infrastructure

List of Symbols

C_u	Coefficient of uniformity
C_c	Coefficient of curvature
D_{\max}	Maximum grain size
D_{10s}	Effective diameter of sand

✉ Abdellah Cherif Taiba
a.cheriftaiba@univ-chlef.dz

D_{10m}	Effective diameter of mixtures
D_{50s}	Mean grain size of sand
D_{50m}	Mean grain size of mixtures
e	Void ratio
e_{max}	Maximum global void ratio
e_{min}	Minimum global void ratio
FA	Fly ash content
G_s	Specific gravity
P_{R10}	Effective particle ratio [$P_{R10} = (D_{10s} - D_{10m})/D_{10s}$]
P_{R50}	Mean particle ratio [$P_{R50} = (D_{50s} - D_{50m})/D_{50s}$]
SP	Poorly graded sand
S_r	Degree of saturation
USCS	Unified Soil Classification System
w	Water content
w_{opt}	Optimum water content
γ_d	Dry density
γ_{dmax}	Maximum dry density
σ_n	Normal stress
τ	Shear stress
τ_{max}	Maximum shear stress
ϕ_{max}	Maximum friction angle

1 Introduction

Soil mechanics deals with the characterization, classification, and eventually improvement of the soil properties involved in civil engineering projects, road infrastructures, and hydraulics embankments. It also studies different problems of instability and deformation of various types of granular soil masses due to the effects of applied initial loading conditions. In addition, it allows the engineers and builders to estimate the strength of soils and improve certain characteristics as well as treat and reinforce these soils for various construction purposes (Meyerhof 1970). Therefore, the assessment of geotechnical engineering characteristics of improved or treated soils used as construction materials for road infrastructure application purposes becomes a real challenge, where the main objective is to increase the shear resistance and/or stability of soil and decrease the project cost considering advantages of the available local materials (Akacem et al. 2019). Indeed, the improvement or treatment of granular materials might be done by changing their properties mechanically (Gu and Lee 2002; Bo et al. 2009; Feng et al. 2011), chemically (Latifi et al. 2017; Galaa et al. 2018; Liu et al. 2019), and by mixing these materials with other soils (Kim et al. 2018; Sabbar et al. 2017) or with bitumen and cement (Ayininuola and Abidoye 2018), pozzolan, and lime (Abbasi and Mahdih 2018). On the other hand, the compaction procedure is the most common method that has been considered in the geotechnical engineering field for improving the soil characteristics to be used in many construction works such as road and railway embankments, dams, landfills, airfields, foundations, and hydraulic barriers. The applied technique can be understood as a procedure that causes reduction of soil volume without variation in its water or mass content; therefore, it is a process that

essentially alters soil structure. A standard Proctor test (ASTM D698-91 1995) is a compaction laboratory test widely used to characterize a borrowed pit and control field compaction characteristics. Therefore, the evaluation of the compaction response of the soil used as construction materials remains a crucial step in the road infrastructure applications for the purpose to avoid eventual subsidence of the soil. Many factors, such as soil type (Gomez et al. 2002), level of compaction (Sanchez et al. 2006), compactive effort, and particle shape, may affect the compaction behavior of soils (Cho et al. 2006; Cherif Taiba et al. 2018, 2019c).

Many other behaviors of soils, such as shear strength (Wang et al. 2013; Cherif Taiba et al. 2016; Mahmoudi et al. 2018, 2020), compressive deformation, hydraulic conductivity (Wang et al. 2012), angle of repose (Wang et al. 2013), and even fracture response (Wang et al. 2007), may also be influenced by soil density and/or water content. The micro-structure of the soil during the loading process may be influenced by several other parameters, such as the applied stresses, the initial gradation of the tested soil (Coop et al. 2004; Cherif Taiba et al. 2017), and the variation of the water content (Mahmoudi et al. 2016a, b, 2019). On the other hand, Doumi et al. (2017) found that the silt content could affect the compaction response of silty sand soils by increasing the maximum dry density and decreasing the optimum water content as the fines content increases from $F_c = 0\%$ to $F_c = 30\%$. The reason behind this improvement is that the fine particles of silt filled the gaps in between the coarse particles of sand and induced a significant increase of the dry density of sand-silt mixtures under consideration. However, Channshetty et al. (2018) studied the influence of fiber content on the compaction of sand-fiber mixtures for the fiber content (UFC = 0.5%, 1%, 2%, and 3%). They observed that the addition of fiber induced a noticeable decrease of the maximum dry density of the tested materials.

On the other hand, the shear strength of soils is one of the most important aspects used to analyze the soil stability problems, such as pavements and embankments, bearing capacity of shallow and deep foundations (Cherif Taiba et al. 2014). Published literature indicated that many studies have been carried out to study the impact of different parameters on the shear strength response of granular soils as sample preparation technique, sample size, confining pressure, stress history, pre-shearing and loading conditions (Yilmaz et al. 2008; Janalizadeh et al. 2013; Belkhatir et al. 2014; Mahmoudi et al. 2016a, b). Hence, particle shape and size were widely considered as vital parameters governing the shear strength characteristics of soils. Wei and Yang (2014), Borhani and Fakharian (2016), Alshibli and Mehmet (2018), Cherif Taiba et al. (2018, 2019a, b), and Xiao et al. (2019) found that these two parameters appeared as determining factors in the characterization and prediction of the mechanical behavior of the granular soils under study.

Moreover, fly ash is one of the most common materials that have been used in the improvement of the mechanical performance in terms of compaction characteristics and shear strength response of soft and expansive soils like clay (Phanikumar and Nagaraju 2018; Nawagamuwa 2018). Saeid et al. (2012) indicated that the fly ash product increased the shear resistance and contributed in the stabilization of subgrade support ability of soils used in the transportation infrastructures as construction materials. Keramatikeman et al. (2017) observed that the increase of the fly ash content induced a higher resistance to liquefaction of granular soils. Phanikumar and Nagaraju (2018) performed a series of compaction tests on clay-fly ash mixtures with varying fly ash

contents (FA = 0%, 10%, 20%, and 30%). They showed that the increase of fly ash content from FA = 0% to FA = 30% induced a very significant decrease in the compaction characteristics in terms of the maximum dry density and optimal water content of clay-fly ash mixtures. Nawagamuwu (2018) studied the effect of fly ash content on the compaction properties of sludge with a range of fly ash (FA = 0–50%). They found that the maximum dry density increased with increasing of fly ash until a threshold fly ash content (FA_{thre} = 30%) then it decreased with the increase of fly ash content from FA = 30% to FA = 50%. In other words, Keramatikerman et al. (2018) reported that fly ash played a determined role in increasing the undrained shear strength of sand, where they found that the undrained shear strength increased with the increase of fly ash content from FA = 0 to 6% for the tested sand-fly ash mixtures.

In other way, particle size is one of the recommended parameters that must be correctly identified in the assessment of the mechanical and hydraulic behavior of granular soils in terms of compaction, shear strength, compressibility, hydraulic conductivity, etc. Thus, very limited researches have been reported to investigate the influence of particle size on the mechanical performance in terms of compaction and shear strength of sand-fly ash binary mixtures for being used in road applications and infrastructure projects. For this purpose, a series of standard compaction tests have been undertaken on three distinct granular classes derived from natural Chlef sand having three different maximum grain sizes as “A” maximum grain size ($D_{\max} = 4.0$ mm, “B” $D_{\max} = 2.0$ mm, and “C” $D_{\max} = 0.63$ mm mixed with fly ash content (FA = 0%, 5%, 10%, and 15%). First, the sand-fly ash mixtures were reconstituted with different water contents ranging from $w = 4\%$ to $w = 14\%$ in order to estimate the optimum Proctor coordinates in terms of the maximum dry density and the optimum water content by the standard compaction test (ASTM D698-91 1995; NF P94-093 1999). Thereafter, another series of direct shear tests were carried out on the same selected materials. However, the sand-fly mixtures were reconstituted with the obtained optimum water content. Then, the samples were placed in direct shear box, compacted with the same compaction energy of Proctor test, and subjected to shear process under the normal stress of ($\sigma_n = 100$ kPa).

2 Index Properties of Used Materials and Testing Procedure

2.1 Materials

The experimental protocol involved three different granular classes derived from natural Chlef sand with different extreme particle sizes named as “A” $D_{\max} = 4.0$ mm, “B” $D_{\max} = 2.0$ mm, and “C” $D_{\max} = 0.63$ mm mixed with fly ash ($D_{\max} = 0.08$ mm) content ranging from FA = 0% to FA = 15% resulting in three binary assemblies. Moreover, the tested sand was extracted from liquefied soil deposit areas along the banks of Chlef River. The three granular classes derived from Chlef sand were classified as poorly graded sand (SP) according to the Unified Soil Classification System (USCS). The fly ash material has been provided by the Chlef (Algeria) cement plant. The chemical composition of the fly ash is shown in Table 1. Figure 1 illustrates the materials used in this laboratory investigation. The properties of the tested materials are presented in Tables 2 and 3. The granulometric curve of the fly ash was determined

by hydrometer test giving maximum grain size of $D_{\max} = 0.08$ mm and mean grain size of $D_{50} = 0.015$ mm. The grain size distribution curves of Chlef sand mixed with different fly ash percentages are shown in Fig. 2.

2.2 Laboratory Testing Program

2.2.1 Compaction Tests

The compaction test is widely used in many geotechnical engineering applications for the purpose to increase the density of soil and consequently decreasing the content of the air voids (Ören 2014). In this context, the tested materials have been prepared through the combination of three subclasses of Chlef sand mixed with fly ash considering different water contents ranging from $w = 4\%$ to $w = 14\%$ and subjected to compaction energy in order to estimate the different optimum Proctor coordinates (maximum dry density ($\gamma_{d\max}$), optimal water content (w_{opt})) by the standard Proctor compaction test (ASTM D698-91 1995; NF P94-093 1999). The sand-fly ash mixtures were stocked in plastic bags and left overnight at constant temperature and humidity to ensure a uniform distribution of moisture. The compaction characteristics response of the different soil samples were established using a standard Proctor apparatus which was conducted with the rammer. It is of cylindrical shape with $D = 50.8$ mm in diameter and $H = 114.3$ mm in height, having a weight of 2.5 kg. The used mold has a diameter of $d = 101.6$ mm and a height of $H = 117$ mm. The samples were compacted in three layers with 587 kJ/m^3 of compaction energy and they were subjected to 25 blows per layer with 30.5 cm drop height.

2.2.2 Direct Shear Tests

A series of direct shear tests was carried out on three different granular classes derived from Chlef sand mixed with fly ash fractions ranging from FA = 0% to FA = 15%. The sand-fly ash mixture samples were reconstituted at the obtained optimum water content from the different compaction tests. The tested materials were placed in the shear box of 60 mm × 60 mm and sample height of 25 mm, then compacted with the same energy fewer than 25 blows. The used soils were subjected to a normal stress of $\sigma_n = 100$ kPa. All the direct shear tests in this study were conducted at a constant speed of 1 mm/min. Tables 2 and 3 summarize the compaction characteristics and shear strength response obtained during the current laboratory investigation.

Table 1 Chemical composition of the used fly ash

Components	Alumina (Al ₂ O ₃)	Calcium oxide (CaO)	Iron oxide (Fe ₂ O ₃)	Magnesium oxide (MgO)	Loss on ignition (LOI)	Silica (SiO ₂)	Titanium oxide (TiO ₂)
Percentage (%)	5.13	66.67	3.78	0.47	0.5–3	22.3	0.5



Fig. 1 Granular materials considered in this study. **a** Categories of Chlef sand. **b** Fly ash

Table 2 Compaction and shear strength characteristics of granular classes derived from natural Chlef sand (FA = 0%) and fly ash (FA = 100%)

Index properties of materials	Materials			
	Sand class A	Sand class B	Sand class C	Fly ash
Maximum grain size (D_{max}) (mm)	4.0	2.0	0.63	0.08
Specific gravity (G_s)	2.66	2.64	2.63	3.08
Effective diameter (D_{10}) (mm)	0.180	0.145	0.123	0.0045
Grain size (D_{30}) (mm)	0.345	0.285	0.212	0.009
Mean grain size (D_{50}) (mm)	0.498	0.430	0.321	0.015
Grain size (D_{60}) (mm)	0.574	0.499	0.383	0.02
Coefficient of uniformity (C_u) (-)	3.199	3.441	3.121	4.444
Coefficient of curvature (C_c) (-)	1.158	1.126	0.960	0.900
Maximum global void ratio (e_{max}) (-)	0.750	0.757	0.813	2.114
Minimum global void ratio (e_{min}) (-)	0.507	0.468	0.549	0.914
Void ratio (e) (-)	0.556	0.555	0.594	-
Degree of saturation (S_r) (%)	47.88	45.21	44.28	-
Maximum dry density (γ_{dmax}) (g/cm ³)	1.71	1.70	1.65	-
Optimum water content (w_{opt}) (%)	10.0	9.50	10.0	-
Maximum shear strength (τ_{max}) (kPa)	80.05	73.45	64.97	-
Unified Soil Classification System	SP	SP	SP	Class C
Grain shape	Rounded	Rounded	Rounded	Rounded

Table 3 Compaction and shear strength characteristics of tested sand-fly ash mixtures

Index properties of materials	Maximum grain size D_{\max} (mm)	Sand-fly ash mixtures		
		FA (%)		
		5	10	15
Specific gravity (G_s)	4.0	2.68	2.70	2.72
	2.0	2.66	2.68	2.71
	0.63	2.65	2.67	2.70
Effective diameter (D_{10}) (mm)	4.0	0.157	0.100	0.038
	2.0	0.128	0.085	0.027
	0.63	0.116	0.086	0.030
Grain size (D_{30}) (mm)	4.0	0.341	0.311	0.267
	2.0	0.283	0.276	0.276
	0.63	0.206	0.199	0.195
Mean grain size (D_{50}) (mm)	4.0	0.497	0.483	0.443
	2.0	0.427	0.425	0.419
	0.63	0.319	0.316	0.313
Grain size (D_{60}) (mm)	4.0	0.575	0.569	0.531
	2.0	0.504	0.512	0.530
	0.63	0.381	0.379	0.376
Coefficient of uniformity (C_u) (–)	4.0	3.674	5.674	13.928
	2.0	3.950	6.012	19.511
	0.63	3.284	4.407	12.701
Coefficient of curvature (C_c) (–)	4.0	1.290	1.692	3.530
	2.0	1.247	1.747	5.311
	0.63	0.960	1.215	3.146
Maximum global void ratio (e_{\max}) (–)	4.0	0.724	0.704	0.683
	2.0	0.723	0.713	0.697
	0.63	0.806	0.792	0.781
Minimum global void ratio (e_{\min}) (–)	4.0	0.444	0.397	0.371
	2.0	0.432	0.413	0.395
	0.63	0.518	0.504	0.486
Void ratio (e) (–)	4.0	0.51	0.49	0.49
	2.0	0.53	0.51	0.51
	0.63	0.55	0.54	0.53
Degree of saturation (S_r) (%)	4.0	46.41	45.52	41.88
	2.0	43.56	43.26	39.74
	0.63	43.71	39.50	37.00
Maximum dry density (γ_{dmax}) (g/cm ³)	4.0	1.78	1.81	1.83
	2.0	1.75	1.78	1.80
	0.63	1.71	1.74	1.77
Optimum water content (w_{opt}) (%)	4.0	8.8	8.29	7.5
	2.0	8.6	8.2	7.45

Table 3 (continued)

Index properties of materials	Maximum grain size D_{max} (mm)	Sand-fly ash mixtures		
		FA (%)		
		5	10	15
	0.63	9.1	8.0	7.2
Maximum shear strength (τ_{max}) (kPa)	4.0	92.33	105.22	112.22
	2.0	86.77	91.39	96.48
	0.63	69.78	73.97	77.9

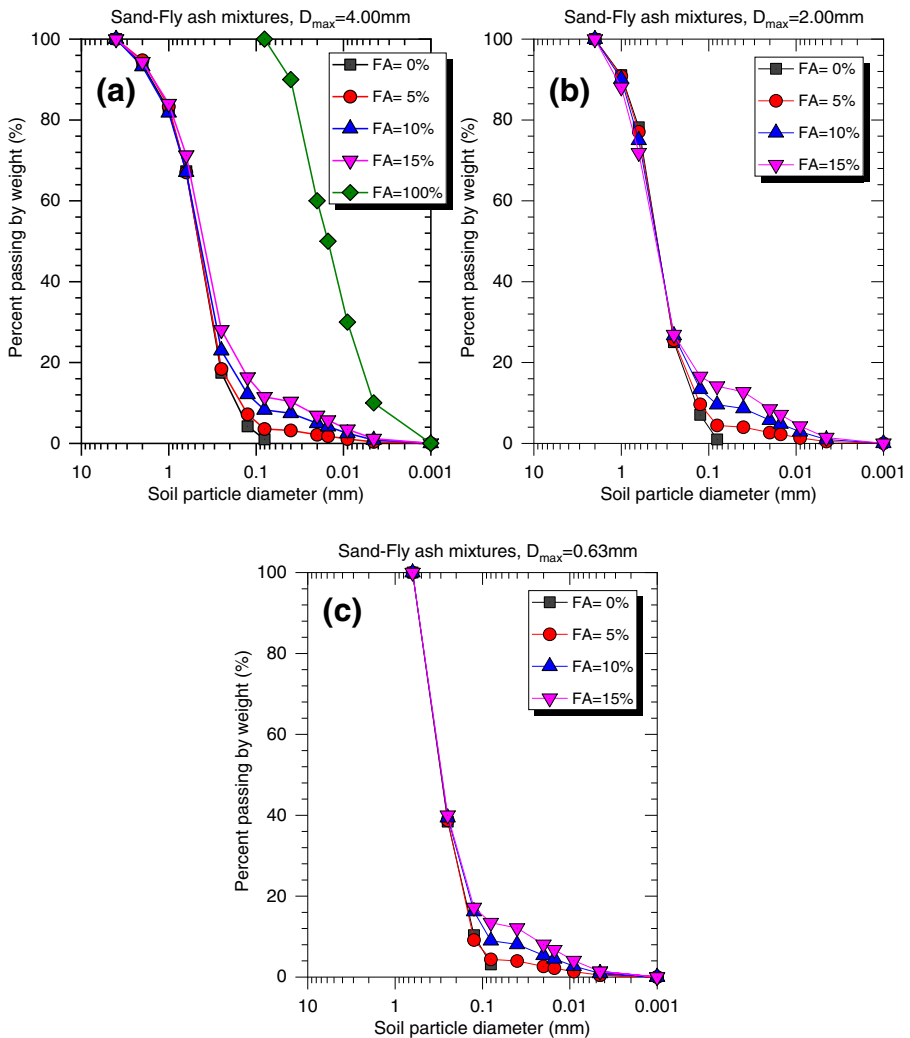


Fig. 2 Grain size distribution curves of tested materials. **a** $D_{max} = 4.0$ mm. **b** $D_{max} = 2.0$ mm. **c** $D_{max} = 0.63$ mm

3 Results and Discussion

3.1 Compaction Results

In order to study the influence of grain size on the compaction of sand-fly ash mixtures, a series of standard compaction tests was carried out on three host granular classes derived from Chlef sand having different maximum sizes ($D_{\max} = 4.0$ mm, 2.0 mm, and 0.63 mm) mixed with fly ash material according to FA ranging between 0% and FA = 15%. The sand-fly ash mixtures were prepared with the range of water content ($w = 4\%$ to $w = 14\%$). Figure 3 shows the evolution of the dry density (γ_d) as a function of water content (w) for the studied materials. According to this figure, it can be seen that the dry density increases with the increase of water content, then it reaches a peak for water contents ranging from $w = 8$ to 10% for clean sands (FA = 0%), from $w = 7\%$ to $w = 11\%$ for the mixtures of FA = 5% and FA = 10%, and from $w = 6\%$ to $w = 9\%$ for the mixtures of FA = 15%. Thereafter, the dry density decreases with the increase of water content for all sand-fly ash mixture samples. Moreover, it is also noted in Fig. 3 that the obtained tendency relating the dry density to the water content increases from the sand-fly ash mixtures with a maximum grain size $D_{\max} = 0.63$ mm, then the mixtures with a maximum grain size $D_{\max} = 2.0$ mm, and finally, the binary of sand-fly ash with a maximum grain size $D_{\max} = 4.0$ mm. This behavior can be explained by the fact that the larger particle sizes play an important role in improving the compaction characteristics of sand-fly ash mixtures compared to the smaller size ones. On the other hand, Fig. 4 presents the effect of fly ash content on the optimum Proctor coordinates of the used tested materials. It is clear from this figure that the fly ash fractions impacted significantly the maximum dry density of the sand-fly ash mixture samples, where the higher values of fly ash content (FA = 15%) exhibit higher values of the optimum Proctor parameters of the studied materials in comparison to the lower values of fly ash fraction (FA = 0%). Moreover, it seems from these figures that the different sand-fly ash mixtures have the trend of shifting the optimum Proctor coordinates (optimum water content and maximum dry density) to the right side in the range of 40 to 60% the degree of saturation.

3.2 Compaction Characteristics Response ($\gamma_{d\max}$, w_{opt}) Versus Maximum Grain Size and Degree of Saturation

In the context of assessing the compaction response ($\gamma_{d\max}$, w_{opt}) as function of maximum grain size (D_{\max}) and degree of saturation (S_r) of the tested materials, Fig. 5 reproduces the results of the current study. As it can be observed from the plot, the D_{\max} has a significant influence on the optimum Proctor coordinates ($\gamma_{d\max}$ and w_{opt}) of the studied materials. Indeed, the increase of the maximum grain size from $D_{\max} = 0.63$ to 4.0 mm for a given fly ash content leads to a remarkable increase of the $\gamma_{d\max}$ and decrease of the w_{opt} of the sand-fly ash mixtures. The obtained trend could be explained by the fact that the coarse grains were at the origin of the increase of the maximum dry density (MDD) of the materials under consideration.

On the other hand, it seems from the 3D plot that a reversed trend was observed for the variation of the maximum dry density and the optimum water content of the studied materials; indeed, the maximum dry density increases with the decrease of the optimum

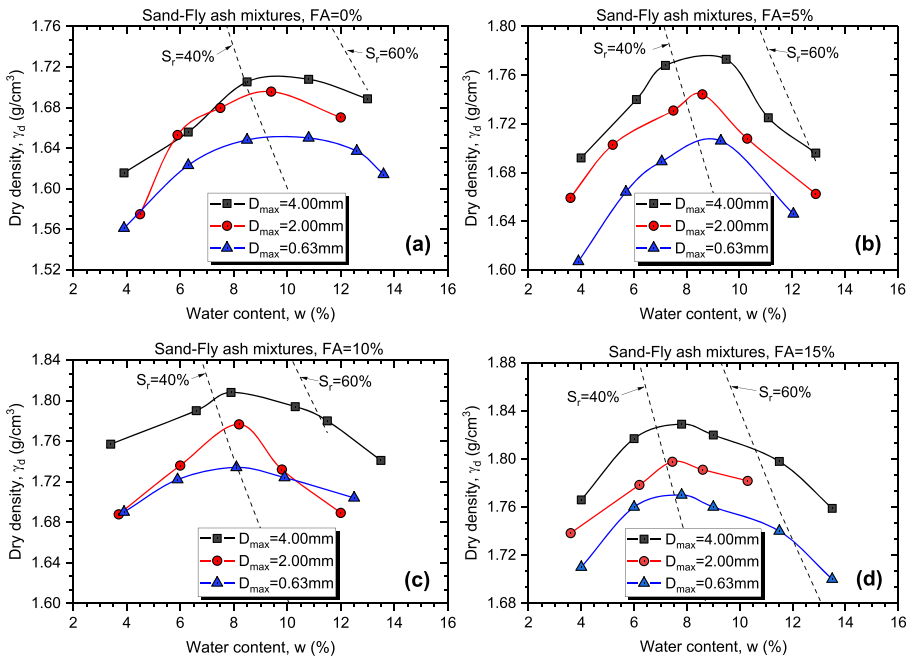


Fig. 3 Dry density versus water content of tested sand-fly ash mixtures. **a** FA = 0%. **b** FA = 5%. **c** FA = 10%. **d** FA = 15%

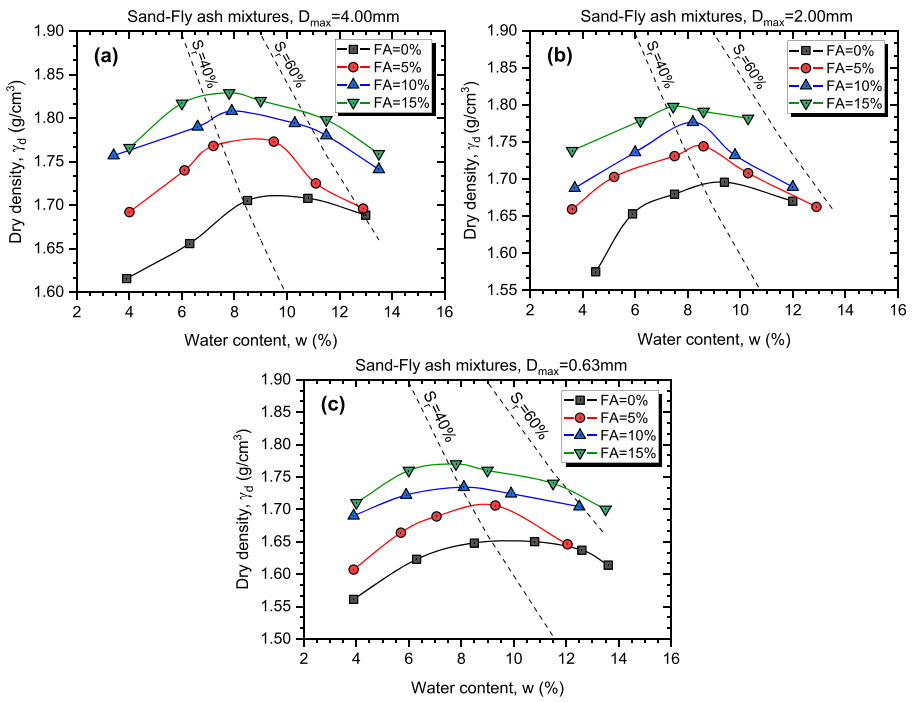


Fig. 4 Dry density versus water content of tested sand-fly ash mixtures. **a** $D_{max} = 4.0$ mm. **b** $D_{max} = 2.0$ mm. **c** $D_{max} = 0.63$ mm

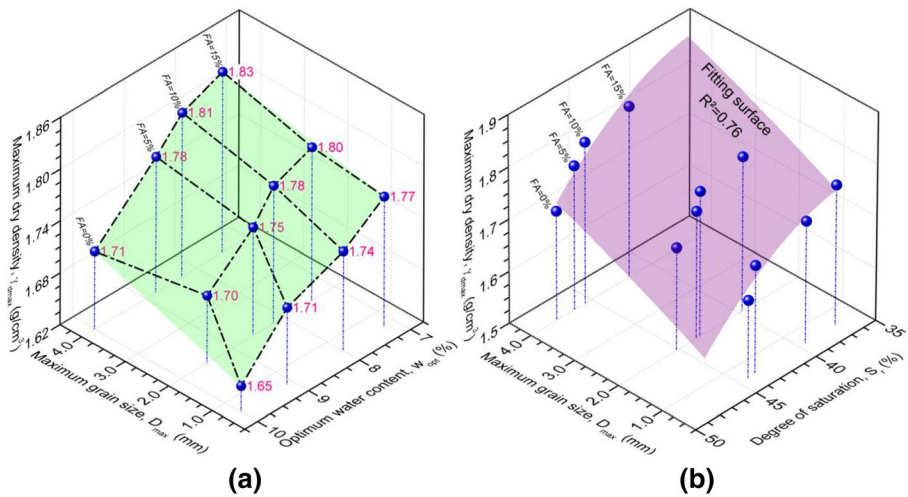


Fig. 5 Variation of maximum dry density as a function of maximum grain size of tested sand-fly ash mixtures. **a** With optimum water content. **b** With degree of saturation

water content of the different sand-fly ash mixtures. This behavior is due to the fact that fine particles of fly ash mixed with the small amounts of water content filling the void spaces between coarse-grained soils cause an increase of the maximum dry density, consequently amplifying the densification states of the tested materials. However, addition of water proportions to the binary mixtures reduce the role of fly ash particles in increasing the optimum Proctor coordinates in terms of the maximum dry density of the materials under study.

Moreover, the relationship between γ_{dmax} , D_{max} , and degree of saturation ($S_r = w * \gamma_s / e * \gamma_w$) is illustrated in Fig. 5b, in which a decrease of degree of saturation at a given maximum grain size leads to a significant increase in the maximum dry density for the different graded sand-fly ash mixture samples for the range of fly ash percentages (FA = 0% to FA = 15%) under consideration. This trend confirm that a good agreement could be established between the γ_{dmax} and the S_r for the different maximum grain sizes ($D_{max} = 0.63$ mm to $D_{max} = 4.0$ mm) with acceptable coefficient of determination ($R^2 = 0.76$) for the tested materials.

3.3 Maximum Dry Density as Function of the Maximum Grain Size, Fly Ash Content, and Void Ratio of the Studied Materials

Figure 6 illustrates the variation of γ_{dmax} with the D_{max} and fly ash fraction (FA) of three binary granular mixtures (sand ($D_{max} = 4.0$ mm)-fly ash mixtures; sand ($D_{max} = 2.0$ mm)-fly ash mixtures; and sand ($D_{max} = 0.63$ mm)-fly ash mixtures). The obtained results indicate that the increase of maximum grain size from $D_{max} = 0.63$ mm to $D_{max} = 4.0$ mm and fly ash content from FA = 0% to FA = 15% leads to a significant increase of the maximum dry density for the studied mixtures from $\gamma_{dmax} = 1.65$ g/cm³ to $\gamma_{dmax} = 1.71$ g/cm³ for FA = 0% and from $\gamma_{dmax} = 1.77$ g/cm³ to $\gamma_{dmax} = 1.83$ g/cm³ for FA = 15% respectively. Meanwhile, the values of maximum dry density of the tested materials according to the used maximum grain sizes ($D_{max} = 4.0$ mm, 2.0 mm,

and 0.63 mm) are $\gamma_{dmax} = 1.71 \text{ g/cm}^3$, 1.70 g/cm^3 , and 1.65 g/cm^3 for pure sands (FA = 0%); $\gamma_{dmax} = 1.78 \text{ g/cm}^3$, 1.75 g/cm^3 , and 1.71 g/cm^3 for the mixture of FA = 5%; $\gamma_{dmax} = 1.81 \text{ g/cm}^3$, 1.78 g/cm^3 , and 1.74 g/cm^3 for the mixture of FA = 10%; and $\gamma_{dmax} = 1.83 \text{ g/cm}^3$, 1.80 g/cm^3 , and 1.77 g/cm^3 for the mixture of FA = 15% respectively. The obtained compaction behavior of the different binary assemblies can be attributed to the increase in the percentage of the fly ash making easier the orientation and movement of particles with adequate size inducing a noticeable decrease of the voids leading to denser state of the tested sand-fly ash mixtures. Moreover, these observations clearly show that the FA and D_{max} play major roles in improving the compaction characteristics of sand-fly ash mixtures and consequently amplifying the soil densification. The outcome of this study is in good agreement with the findings of Saeid et al. (2012), Phanikumar and Nagaraju (2018), and Nawagamuwa (2018).

On the other hand, Fig. 6b demonstrates clearly the relationship between maximum dry density and void ratio for a given maximum grain size of the tested sand-fly ash mixtures for the range of fly ash content from FA = 0% to FA = 15%. It seems that the fitting surface could well capture the relationship between the maximum dry density and the void ratio ($R^2 = 0.97$) for all the materials under consideration. Indeed, it increases with the decrease of the void ratio for the various maximum grain sizes. This behavior indicates that the increase of the maximum dry density leads to minimize the void spaces between coarse-fine particles and consequently increasing the densification state of the sand-fly ash mixture samples under study. Equation (1) is proposed to represent the variation of the γ_{dmax} as a function of the D_{max} and FA of the tested materials:

$$\gamma_{dmax} = 0.004 \times (D_{max})^2 + 0.04 \times (D_{max}) - 0.0003 \times (FA)^2 + 0.01 \times (FA) + 1.63 \quad (1)$$

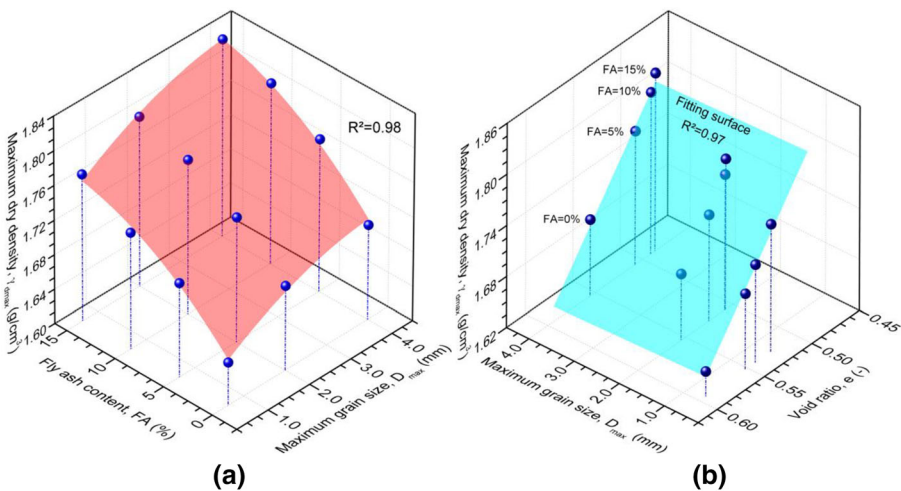


Fig. 6 Maximum dry density (γ_{dmax}) versus maximum grain size (D_{max}) of the tested materials. **a** With fly ash. **b** With void ratio

3.4 Correlation Between the Maximum Dry Density and Particle Ratios of Tested Sand-Fly Ash Mixtures

For the purpose to identify clearly the influence of particle size on the optimum Proctor coordinates of sand-fly ash mixtures, two new parameters named as effective particle ratio (P_{R10}) and mean particle ratio (P_{R50}) were introduced according to the following equations:

$$P_{R10} = \frac{D_{10s} - D_{10m}}{D_{10s}} \quad (2)$$

$$P_{R50} = \frac{D_{50s} - D_{50m}}{D_{50s}} \quad (3)$$

where D_{10s} is effective diameter of sand, D_{50s} is mean grain size of sand, D_{10m} is effective diameter of mixtures, and D_{50m} is mean grain size of mixtures.

3.4.1 Influence of the P_{R10}

Figure 7 shows the variation of the γ_{dmax} as a function of the effective particle ratio of three granular classes derived from Chlef sand having different maximum grain sizes as $D_{max} = 0.63$ mm; $D_{max} = 2.0$ mm; and $D_{max} = 4.0$ mm mixed with 0%, 5%, 10%, and 15% of fly ash material. The obtained results indicate that the maximum dry density could be correlated with the effective particle ratio of the tested sand-fly ash mixtures. In addition, it increases according to a polynomial function with the increase of the effective particle ratio for all tested materials. Moreover, it could be seen from Fig. 7 that the effective particle ratio of sand-fly ash mixtures exhibits higher values for the granular class characterized with the maximum grain size ($D_{max} = 4.0$ mm) compared to the other two granular classes ($D_{max} = 2.0$ mm and $D_{max} = 0.63$ mm). This increase may result from the role of the fly ash fraction in increasing the effective particle ratio of different graded sand-fly ash mixtures leading to an increase of the densification state of the binary mixtures for the considered maximum grain size. Furthermore, the obtained results demonstrate clearly that the maximum dry density correlates very well ($0.88 \leq R^2 \leq 0.96$) with the P_{R10} according to the following equations:

For the mixtures $4.0 \text{ mm} \leq D_{max} \leq 0.001$ mm:

$$\gamma_{dmax} = -0.26 \times (P_{R10})^2 + 0.34 \times (P_{R10}) + 1.72 \text{ with } R^2 = 0.94 \quad (4)$$

For the mixtures $2.0 \text{ mm} \leq D_{max} \leq 0.001$ mm:

$$\gamma_{dmax} = -0.20 \times (P_{R10})^2 + 0.28 \times (P_{R10}) + 1.70 \text{ with } R^2 = 0.97 \quad (5)$$

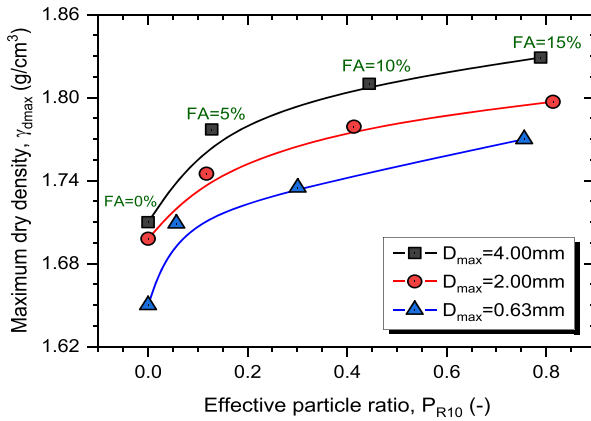


Fig. 7 Maximum dry density versus effective particle ratio (P_{R10}) of tested sand-fly ash mixtures

For the mixtures $0.63 \text{ mm} \leq D_{max} \leq 0.001 \text{ mm}$:

$$\gamma_{dmax} = -0.25 \times (P_{R10})^2 + 0.32 \times (P_{R10}) + 1.67 \text{ with } R^2 = 0.88 \tag{6}$$

3.4.2 Influence of the Mean Particle Ratio

The effect of the P_{R50} on the γ_{dmax} of the sand-fly ash binary assemblies is presented in Fig. 8. It is observed from this figure that the maximum dry density correlates very well ($0.77 \leq R^2 \leq 0.99$) with the mean particle ratio according to a polynomial function for the tested materials. Therefore, the maximum dry density increases with the increase of mean particle ratio. On the other hand, it is clearly shown in Fig. 8 that the trend between maximum dry density and mean particle ratio exhibited higher values for the coarser sand ($D_{max} = 4.0 \text{ mm}$)-fly ash mixtures compared to both the medium sand ($D_{max} = 2.0 \text{ mm}$)-fly ash mixtures and the finer sand ($D_{max} = 0.63 \text{ mm}$)-fly ash mixtures. The obtained tendency can be explained by the fact that the increase in the maximum grain size from $D_{max} = 0.63 \text{ mm}$ to $D_{max} = 4.0 \text{ mm}$ leads to a significant increase of the mean particle ratio affecting considerably the amplification of the maximum dry density of the tested materials. The following expressions are suggested to evaluate the γ_{dmax} as a function of the P_{R50} for the tested sand-fly ash mixtures:

For the mixtures $4.0 \text{ mm} \leq D_{max} \leq 0.001 \text{ mm}$:

$$\gamma_{dmax} = -20.37 \times (P_{R50})^2 + 3.06 \times (P_{R50}) + 1.74 \text{ with } R^2 = 0.77 \tag{7}$$

For the mixtures $2.0 \text{ mm} \leq D_{max} \leq 0.001 \text{ mm}$:

$$\gamma_{dmax} = -200.42 \times (P_{R50})^2 + 9.07 \times (P_{R50}) + 1.70 \text{ with } R^2 = 0.99 \tag{8}$$

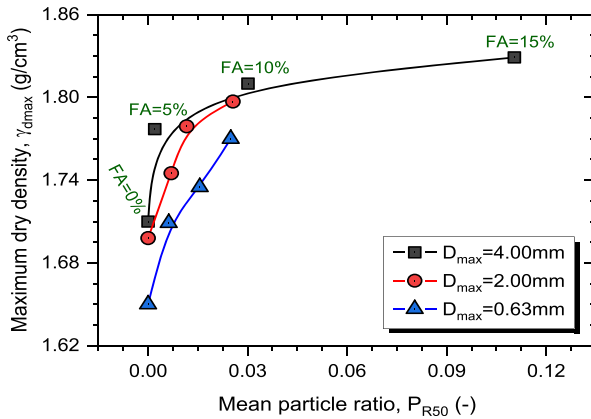


Fig. 8 Maximum dry density versus mean particle ratio (P_{R50}) of tested sand-fly ash mixtures

For the mixtures $0.63 \text{ mm} \leq D_{max} \leq 0.001 \text{ mm}$:

$$\gamma_{dmax} = -128.28 \times (P_{R50})^2 + 7.70 \times (P_{R50}) + 1.66 \text{ with } R^2 = 0.97 \quad (9)$$

3.5 Shear Strength Response

A series of direct shear tests was carried out on different sand-fly ash mixture samples reconstituted with the obtained optimum Proctor coordinates γ_{dmax} and w_{opt} as follows: $w_{opt} = 9.5$ to 10% for clean sand $FA = 0\%$; from $w_{opt} = 8$ to 9.1% for the $FA = 5\%$ mixtures; from $w_{opt} = 8$ to 8.29% for the $FA = 10\%$ mixtures; and from $w_{opt} = 7.2$ to 7.5% for the $FA = 15\%$ mixtures respectively. Moreover, the samples were placed in direct shear box with $60 \text{ mm} \times 60 \text{ mm} \times 25 \text{ mm}$, reconstituted with the same procedure as the Proctor test and subjected to a normal stress of $\sigma_n = 100 \text{ kPa}$.

Figures 9, 10, 11, and 12 illustrate the mechanical behavior of three granular classes derived from Chlef sand having different maximum grain sizes ($D_{max} = 4.0 \text{ mm}$, 2.0 mm , and 0.63 mm) mixed with the fraction of fly ash ranging between $FA = 0\%$ and $FA = 15\%$. It is clear from the outcome of this laboratory investigation that the particle size in terms of the maximum grain size has a major effect on the shear strength of the tested materials. Indeed, the $D_{max} = 4.0 \text{ mm}$ sand-fly ash mixtures exhibit the highest shear strength (maximum shear stress (τ_{max}) = 80.05 kPa , 92.33 kPa , 105.22 kPa , and 112.22 kPa) compared to the $D_{max} = 2.0 \text{ mm}$ sand-fly ash mixtures ($\tau_{max} = 73.45 \text{ kPa}$, 86.77 kPa , 91.39 kPa , and 96.48 kPa) and the $D_{max} = 0.63 \text{ mm}$ sand-fly ash mixtures ($\tau_{max} = 64.97 \text{ kPa}$, 69.78 kPa , 73.97 kPa , and 77.90 kPa) for the tested fly ash contents ($FA = 0\%$, $FA = 5\%$, $FA = 10\%$, and $FA = 15\%$) respectively. This behavior can be attributed to the impact of the maximum grain size parameter enabling the particles of fly ash to increase the intergranular contacts leading to the increase of the interlocking and consequently increasing dilativeness of the first category of mixtures compared to the other two granular classes of sand-fly ash mixtures under consideration. These findings are in good agreement with the obtained results by Keramatikerman et al. (2017), Keramatikerman et al. (2018), and Kolay et al. (2019). In addition, the plot of the vertical displacement versus horizontal displacement clearly

shows the role of the maximum grain size (D_{max}) to increase the dilative character for the tested parameters and consequently leading to the increase of shear resistance due to the increase of the interlocking of the tested materials as illustrated in Figs. 9b, 10b, 11b, and 12b.

3.6 Combined Effects of the D_{max} and w_{opt} on the Maximum Shear Strength of the Tested Materials

The combined effects of the D_{max} and optimum water content (w_{opt}) on the τ_{max} of three granular classes of sand mixed with various percentages of fly ash (FA = 0%, 5%, 10%, and 15%) are illustrated in Fig. 13. As it can be seen, the obtained results indicate that the optimum water content and maximum grain size have noticeable effects on the maximum shear strength of sand-fly ash binary matrix. Indeed, the τ_{max} increases in a linear manner with the decrease of the optimal water content through the range of $w_{opt} = 10\%$ to $w_{opt} = 7\%$ for all the tested materials. This behavior confirms that the amplification of water content leads to widen the gaps within the texture of the sand-fly ash mixture matrix structure and consequently giving rise to much more unstable samples. In other terms, the particle size parameter has a remarkable impact on the maximum shear strength of the selected materials. This trend is clearly observed for sand-fly ash mixtures with a maximum grain size ($D_{max} = 4.0$ mm) compared to that of the sand ($D_{max} = 2.0$ mm)-fly ash mixtures and the sand ($D_{max} = 0.63$ mm)-fly ash mixtures respectively. Moreover, it is clearly seen from the 3D plot that there exists a good correlation between the particle size in terms of the maximum grain size and the optimum water content of the sand-fly ash mixture samples, where the optimum water content decreases in a linear manner with the increase of maximum grain size for all the tested materials.

3.7 Maximum Shear Strength as Function of the Maximum Grain Size and Fly Ash Content

Figure 14 illustrates the evolution of the τ_{max} as a function of the D_{max} and fly ash content (FA) of the three different graded sand-fly ash binary assemblies. As it can be

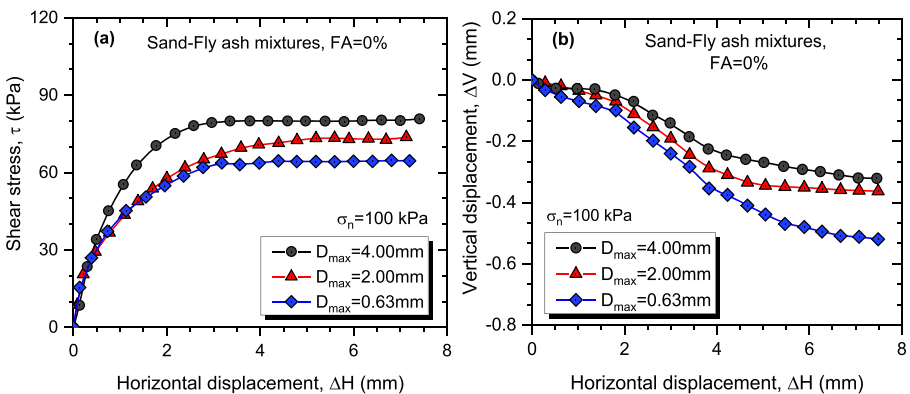


Fig. 9 Influence of maximum grain size on the mechanical behavior of the sand-fly ash mixtures (FA = 0%). **a** Shear stress as a function of horizontal displacement. **b** Vertical displacement as a function of horizontal displacement

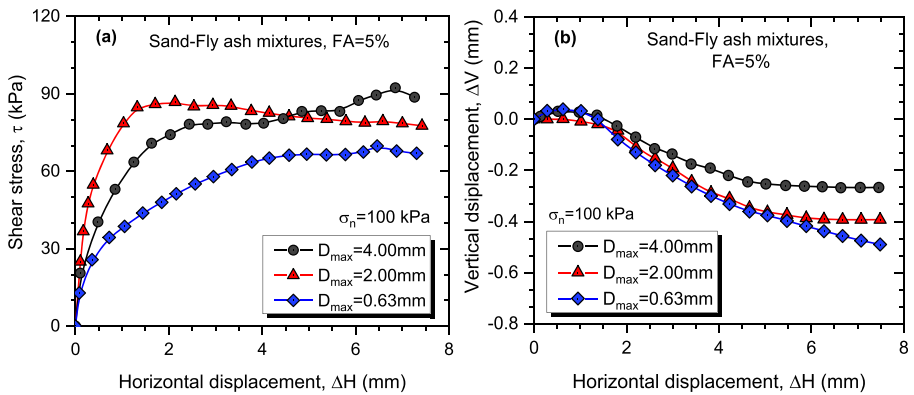


Fig. 10 Influence of maximum grain size on the mechanical behavior of the tested sand-fly ash mixtures (FA = 5%). **a** Shear stress versus horizontal displacement. **b** Vertical displacement versus horizontal displacement

seen from the 3D plot, the maximum grain size and fly ash content have noticeable impact on improving of the maximum shear strength of the studied mixtures. Indeed, the maximum shear strength decreases with the decrease of the maximum grain size ($D_{max} = 4.0$ mm, 2.0 mm, and 0.63 mm) and tested fly ash contents (FA = 0%, FA = 5%, FA = 10%, and FA = 15%) for the sand-fly ash mixtures under study: $\tau_{max} = 80.05$ kPa, 73.45 kPa, and 64.97 kPa for clean sands (FA = 0%); $\tau_{max} = 92.33$ kPa, 86.77 kPa, and 69.78 kPa for the FA = 5% mixture; $\tau_{max} = 105.22$ kPa, 91.39 kPa, and 73.97 kPa for the FA = 10% mixture; and $\tau_{max} = 112.22$ kPa, 96.48 kPa, and 77.90 kPa for the FA = 15% mixture respectively. This behavior is due to the effective existence of fly ash fines in-between coarse-sand particles favorizing a dilative character of the sand-fly ash mixtures resulting in more stable structure of the sand-fly ash matrix under study. The obtained results confirm the role of the particle size and fly ash fraction in improving the shear strength of granular materials for being used in transportation infrastructure applications. The results, thus, obtained are in agreement with the findings of Keramatikeman et al. (2017), Keramatikerman et al. (2018), and Kolay et al. (2019).

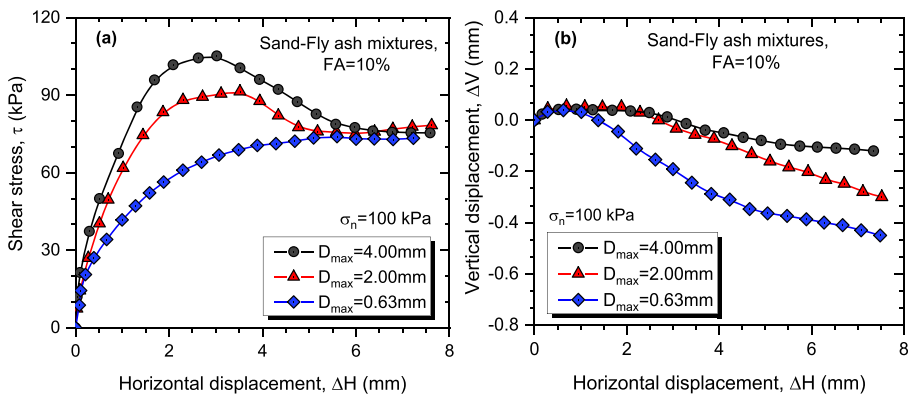


Fig. 11 Influence of maximum grain size on the mechanical behavior of the sand-fly ash mixtures (FA = 10%). **a** Shear stress versus horizontal displacement. **b** Vertical displacement versus horizontal displacement

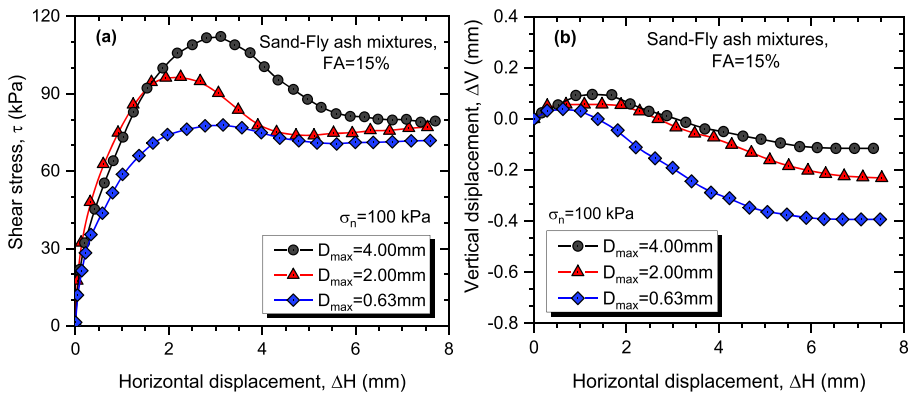


Fig. 12 Influence of maximum grain size on the mechanical behavior of the sand-fly ash mixtures (FA = 15%). **a** Shear stress versus horizontal displacement. **b** Vertical displacement versus of horizontal displacement

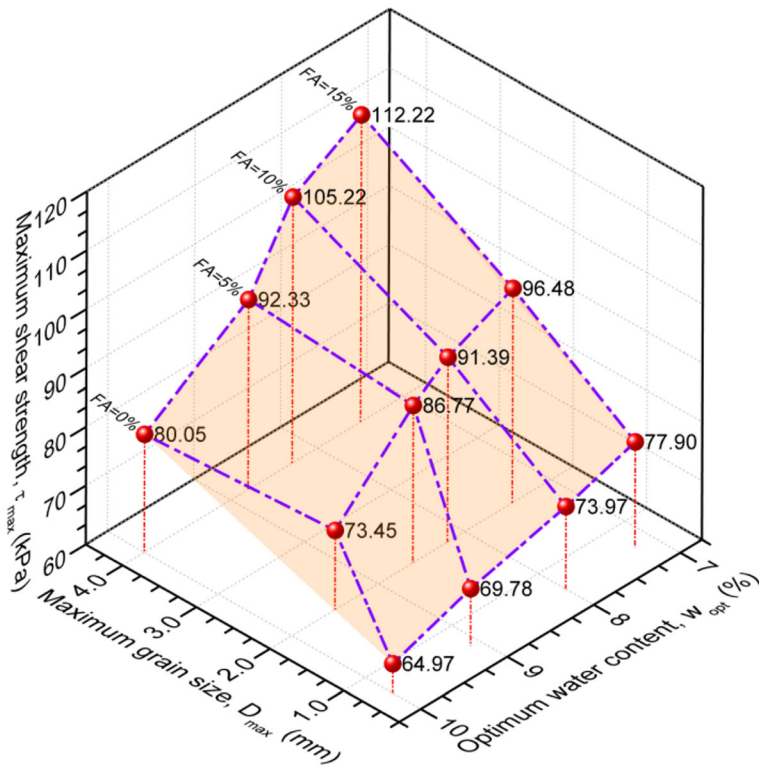


Fig. 13 Maximum shear strength versus maximum grain size and optimum water content for the tested sand-fly ash mixtures

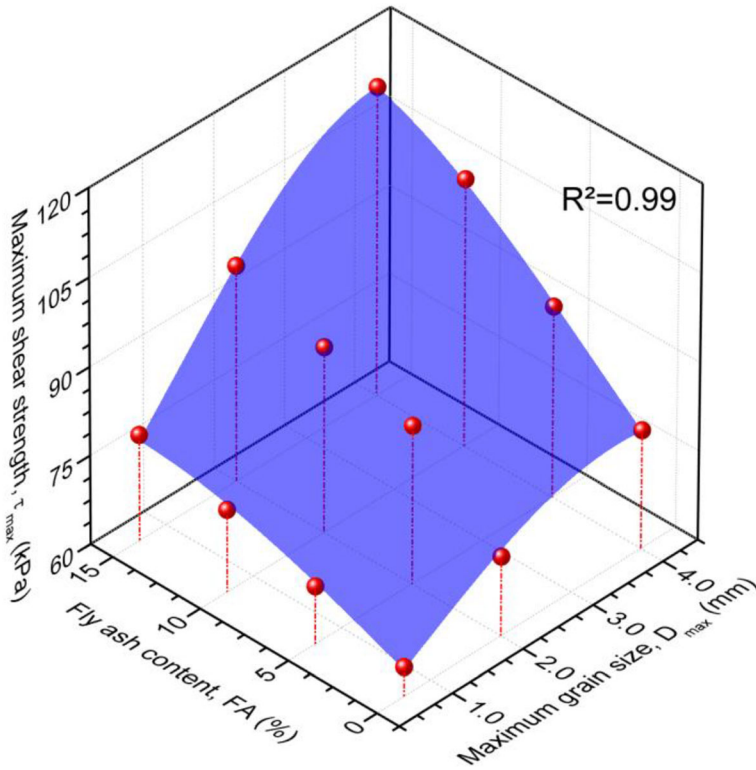


Fig. 14 Variation of maximum shear strength with maximum grain size and fly ash content of the tested materials

3.8 Correlation Between the Maximum Shear Strength and Particle Ratios of Tested Sand-Fly Ash Mixtures

3.8.1 Influence of the Effective Particle Ratio

For the purpose to study the influence of the effective particle ratio (P_{R10}) on the maximum shear strength of three distinct binary assemblies having different maximum grain sizes ($D_{max} = 4.0$ mm, 2.0 mm, and 0.63 mm), Fig. 15 reproduces the test results obtained from the current study. It is clear from this figure that the effective particle ratio has a remarkable effect on the maximum shear strength of the tested materials, where the maximum shear strength increases polynomially with the increase of the effective particle ratio for the tested sand ($D_{max} = 4.0$ mm)-fly ash mixtures, sand ($D_{max} = 2.0$ mm)-fly ash mixtures, and sand ($D_{max} = 0.63$ mm)-fly ash mixtures. Moreover, it is clearly observed from Fig. 15 that for the different graded sand-fly ash mixtures, the higher effective particle ratio (higher fly ash content “FA = 15%”) exhibits higher maximum shear strength compared to the lower effective particle ratio (lower fly ash content “FA = 0%”) indicating a lower maximum shear strength. The obtained data confirm a reliable relationship between the maximum shear strength and effective particle ratio of the sand-fly ash mixture samples under consideration. The following expression is proposed to evaluate the maximum shear strength (τ_{max}) as a

function of the P_{R10} of the tested materials:

$$\tau_{\max} = a \times (P_{R10})^2 + b \times (P_{R10}) + c \tag{10}$$

Table 4 shows the coefficients a , b , and c and the corresponding coefficient of determination (R^2) for the material under consideration.

3.8.2 Influence of the Mean Particle Ratio

The influence of the mean particle ratio [$P_{R50} = (D_{50s} - D_{50m})/D_{50s}$] on the τ_{\max} of three different classes of Chlef sand-fly ash mixtures is presented in Fig. 16. As it can be seen, the data illustrated in this plot indicate that the mean particle ratio could be considered as appropriate parameter to predict the shear strength characteristics (τ_{\max} and P_{R50}) of the tested soil samples. Indeed, the maximum shear strength increases with the increase of the mean particle ratio for the selected materials and a good polynomial relationship ($R^2 \geq 0.91$) may relate the two characteristics of the sand-fly ash binary matrix. Moreover, the test results show that the coarser sand ($D_{\max} = 4.0$ mm)-fly ash mixtures exhibited higher values of the maximum shear strength and mean particle ratio compared to the medium sand ($D_{\max} = 2.0$ mm)-fly ash mixtures and finer sand ($D_{\max} = 0.63$ mm)-fly ash mixtures. This tendency confirms that coarser sand particles ($D_{\max} = 4.0$ mm) mixed with the fly ash materials were at the origin of increasing the mean particle ratio of mixtures leading to the increase of the maximum shear strength of these mixtures in comparison to the mixtures reconstituted from the medium and finer sand particles ($D_{\max} = 2.0$ mm and $D_{\max} = 0.63$ mm) and fly ash under consideration. The following equation is suggested to correlate the τ_{\max} to the P_{R50} of the tested materials:

$$\tau_{\max} = a \times (P_{R50})^2 + b \times (P_{R50}) + c \tag{11}$$

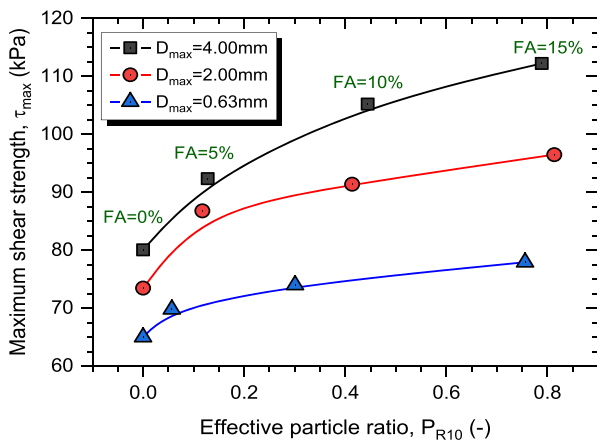


Fig. 15 Maximum shear strength versus effective particle ratio (P_{R10}) of tested sand-fly ash mixtures

Table 4 Coefficients a , b , and c and R^2 for Eq. (8)

Sand-fly ash mixtures	a	b	c	R^2
$4.0 \text{ mm} \leq D_{\max} \leq 0.001 \text{ mm}$	-50.66	78.96	81.18	0.99
$2.0 \text{ mm} \leq D_{\max} \leq 0.001 \text{ mm}$	-43.96	60.31	76.06	0.90
$0.63 \text{ mm} \leq D_{\max} \leq 0.001 \text{ mm}$	-26.41	35.35	66.21	0.95

Table 5 shows the coefficients a , b , and c and the corresponding coefficient of determination (R^2) for the material under consideration.

3.9 Maximum Friction Angle as Function of the Maximum Grain Size and Fly Ash Content

The variation of the maximum (peak) friction angle [$\phi_{\max} = \tan^{-1}(\tau_{\max}/\sigma_n)$] with maximum grain size and fly ash content of the tested materials is shown in Fig. 17. As seen from this figure, the maximum grain size and fly ash content have a noticeable effect on the maximum friction angle of the binary mixtures under study. Indeed, an increase in the fly ash content from FA = 0% to FA = 15% at a given maximum grain size leads to a significant increase in the maximum friction angle of the tested sand-fly ash mixtures. This behavior could be explained by the role of the fly ash particles present in between the coarse sand grain voids to increase the intergranular friction forces leading to the increase of the interlocking and consequently enhancing the shearing characteristics response of the tested soils. Moreover, the increase in the maximum grain size from $D_{\max} = 0.63$ to 4.0 mm contributes significantly in increasing the maximum friction angle by 17.2%, 22.4%, 27.3%, and 27.4% for the fly ash contents (FA = 0%, 5%, 10%, and 15%) respectively.

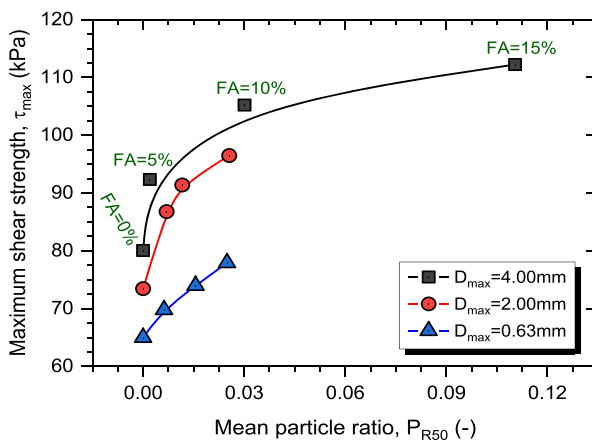
**Fig. 16** Maximum shear strength versus mean particle ratio of different classes of Chlef sand-fly ash mixtures

Table 5 Coefficients *a*, *b*, and *c* and *R*² for Eq. (9)

Sand-fly ash mixtures	<i>a</i>	<i>b</i>	<i>c</i>	<i>R</i> ²
4.0 mm ≤ <i>D</i> _{max} ≤ 0.001 mm	− 54.64	84.86	85.12	0.91
2.0 mm ≤ <i>D</i> _{max} ≤ 0.001 mm	− 48.61	21.34	73.63	0.99
0.63 mm ≤ <i>D</i> _{max} ≤ 0.001 mm	− 86.95	72.31	65.17	0.99

4 Conclusion

Particle size characteristics and fly ash material play an important role in the evaluation of the mechanical performance of granular materials; therefore, they should be included in developed models to better predict the outcome of the compaction process and shear strength characteristics in order to identify the combined effects of the two parameters on the shear strength of sand-fly ash mixtures for the purpose to valorize granular materials in road applications and embankment projects. This paper includes an analysis of the compaction and shear strength of granular materials considering the influence of particle size and fly ash content on the resulted characteristics in terms of the maximum dry density, the optimum water content, and the maximum shear strength of sand-fly ash mixtures. The study is based on the use of three different granular classes derived from natural Chlef sand having different maximum particle sizes such as *D*_{max} = 4.0 mm, 2.0 mm, and 0.63 mm mixed with a fraction of fly ash ranging from FA = 0% to FA = 15%. The main conclusions are summarized below:

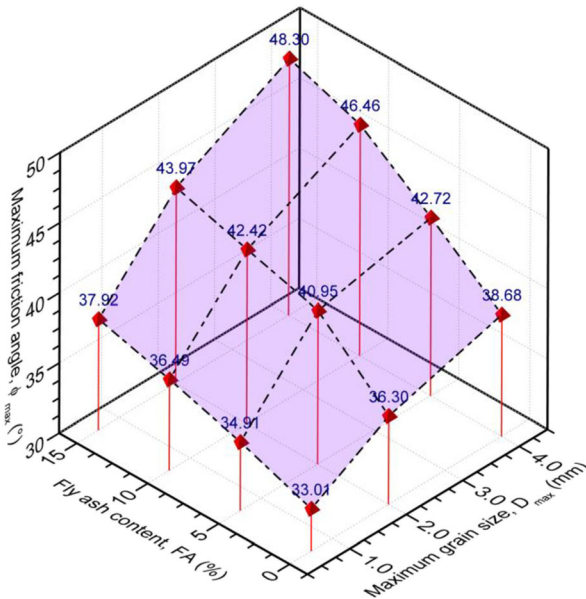


Fig. 17 Maximum friction angle as a function of maximum grain size and fly ash content of tested sand-fly ash mixtures

- 1- The obtained data indicate the maximum particle size (D_{\max}) and fly ash content (FA) have remarkable influences on the optimum Proctor coordinates in terms of maximum dry density " γ_{dmax} " and optimum water content " w_{opt} " of the tested sand-fly ash binary mixtures. Moreover, the addition of the fly ash fraction from FA = 0% to FA = 15% to the granular soil induces an increase in the maximum dry density and decrease in the optimum water content. In other terms, the increase of the maximum diameter from $D_{\max} = 0.63$ mm to $D_{\max} = 4.0$ mm leads to a significant increase of the maximum dry density of the tested sand-fly ash binary assemblies. This means that the distribution of the coarse particles contribute effectively to the amplification of the densification state of the sand-fly ash mixtures. The outcome of this study is in good agreement with the findings of Saeid et al. (2012), Phanikumar and Nagaraju (2018), and Nawagamuwa (2018).
- 2- The test results show that the consideration of particle size characteristic in the reconstitution of coarse-grained soil samples treated with the fly ash material has an effective impact on the enhancement of the mechanical behavior in terms of the maximum shear strength of the tested materials. Therefore, the increase of the maximum diameter (D_{\max}) and fly ash content (FA) induces an important increase of the maximum shear strength (τ_{\max}) of the tested binary mixtures. However, the maximum shear strength continues to decrease with the increase of the optimum water content of the selected materials. This behavior confirms that higher values of water contents lead to more compressible sand-fly ash mixtures and consequently giving rise to a more unstable structure of the samples. These findings are in good agreement with the obtained results by Keramatikeman et al. (2017), Keramatikerman et al. (2018), and Kolay et al. (2019).
- 3- The outcome of this experimental investigation indicates that the new introduced particle size ratio characteristics named as effective particle ratio $P_{R10} = (D_{10s} - D_{10m})/D_{10s}$ and mean particle ratio $P_{R50} = (D_{50s} - D_{50m})/D_{50s}$ appear as suitable factors to predict the mechanical performance of the sand-fly ash mixtures in terms of compaction response and shear strength characteristics in the context to valorize granular soil materials for being used in transportation infrastructure engineering applications. Moreover, the obtained data confirm that the fly ash fraction and the maximum grain size have a noticeable effect on the maximum friction angle of the tested binary granular mixtures.

Acknowledgments This research work was carried out in the Laboratory of Materials Sciences & Environment in the context of a research project between Hassiba Benbouali University of Chlef (Algeria) and Ruhr University of Bochum (Germany). The authors are thankful to all those who effectively contributed to the achievement of this laboratory investigation.

Author Contribution Section All authors have contributed to the conception, writing, and design of the submission manuscript. Material collection, sample preparation, and analysis were performed by Mr. Hamou Azaiez, Dr. Abdellah Cherif Taiba, Dr. Youcef Mahmoudi, and Pr. Mostefa Belkhatir. The first draft of the manuscript was written by all authors and they have commented on previous versions of the manuscript. All authors read and approved the final version of the manuscript.

Funding Information The authors are grateful for the financial support received from the Directorate General for Scientific Research and Technological Development, Ministry of Higher Education and Scientific Research (Algeria).

Compliance with Ethical Standards

Conflict of Interest The authors declare that they have no conflict of interest.

References

- Abbasi, N., Mahdich, M.: Improvement of geotechnical properties of silty sand soils using natural pozzolan and lime. *Geo-Eng.* **9**, 4 (2018). <https://doi.org/10.1186/s40703-018-0072-4>
- Akacem, M., Zentar, R., Mekerta, B., Sadok, A., Moulay Omar, H.: Co-valorisation of local materials tuffs and dune sands in construction of roads. *Geotech Geol Eng.* (2019). <https://doi.org/10.1007/s10706-019-01035-4>
- Alshibli, K.A., Mehmet, B.C.: Influence of particle morphology on the friction and dilatancy of sand. *J Geotech Geoenviron Eng.* **144**, 04017118 (2018). [https://doi.org/10.1061/\(ASCE\)GT.1943-5606.0001841](https://doi.org/10.1061/(ASCE)GT.1943-5606.0001841)
- ASTM D698-91 (1995). Standard test methods for laboratory compaction characteristics of soil using standard effort. (12,400 ft-lbf/ft³(600 kN-m/m³)), Annual Book of ASTM Standard, Vol 04.08, ASTM International, West Conshohocken, P A, pp 69-76
- Ayinuola, G.M., Abidoye, S.P.: Soil stabilization using bitumen emulsion and cement combination as additive. *J Earth Sci Eng.* **8**, 66–74 (2018). <https://doi.org/10.17265/2159-581X/2018.02.000>
- Belkhatir, M., Schanz, T., Arab, A., Della, N., Kadri, A.: Insight into the effects of gradation on the pore pressure generation of sand–silt mixtures. *Geotech Test J.* **37**(5), 20130051 (2014). <https://doi.org/10.1520/gtj20130051>
- Bo, M.W., Na, Y.M., Arulrajah, A., Chang, M.F.: Densification of granular soil by dynamic compaction. *Proc Inst Civ Eng - Ground Improvement.* **162**(3), 121–132 (2009). <https://doi.org/10.1680/jgrim.2009.162.3.121>
- Borhani, A., Fakharian, K.: Effect of particle shape on dilative behavior and stress path characteristics of Chamkhaleh sand in undrained triaxial tests. *Int J Civ Eng.* **14**(4), 197–208 (2016)
- Channshetty, J., Prathap Kumar, M.T., Raghunandan, M.E.: Compaction characteristics and strength of BC soil reinforced with untreated and treated coir fibers. *J Innov Infrastruct Solut.* **3**, 21 (2018). <https://doi.org/10.1007/s41062-017-0123-2>
- Cherif Taiba, A., Mahmoudi, Y., Belkhatir, M., Kadri, A., Schanz, T.: Effect of gradation on mechanical behavior of silty sand soils. *Colloque International« Caractérisation et Modélisation des Matériaux et Structures »* (2014)
- Cherif Taiba, A., Mahmoudi, Y., Belkhatir, M., Kadri, A., Schanz, T.: Insight into the effect of granulometric characteristics on static liquefaction susceptibility of silty sand soils. *Geotech Geol Eng.* **34**, 367–382 (2016). <https://doi.org/10.1007/s10706-015-9951-z>
- Cherif Taiba, A., Mahmoudi, Y., Belkhatir, M., Kadri, A., Tom Schanz, T.: [Experimental characterization of the undrained instability and steady state of silty sand soils under monotonic loading conditions.](#) *Int J Geotech Eng.* (2017). <https://doi.org/10.1080/19386362.2017.1302643>
- Cherif Taiba, A., Mahmoudi, Y., Belkhatir, M., Schanz, T.: Experimental investigation into the influence of roundness and sphericity on the undrained shear response of silty sand soils. *Geotech Test J.* **41**, 20170118 (2018). <https://doi.org/10.1520/GTJ20170118>
- Cherif Taiba, A., Mahmoudi, Y., Hazout, L., Belkhatir, M., Baille, W.: Evaluation of hydraulic conductivity through particle shape and packing density characteristics of sand–silt mixtures. *Mar Georesour Geotechnol.* **37**, 1–13 (2019a). <https://doi.org/10.1080/1064119x.2018.1539891>
- Cherif Taiba, A., Mahmoudi, Y., Hazout, L., Belkhatir, M., Baille, W.: Effects of gradation on the mobilized friction angle for the instability and steady states of sand–silt mixtures: experimental evidence. *Acta Geotech Slov.* (2019b). <https://doi.org/10.18690/actageotechslov.16.1.79-95>
- Cherif Taiba, A., Mahmoudi, Y., Belkhatir, M., Baille, W.: Assessment of the correlation between grain angularity parameter and friction index of sand containing low plastic fines. *Geomech Geoeng.* 1–17 (2019c). <https://doi.org/10.1080/17486025.2019.1648881>
- Cho, G.-C., Dodds, J., Santamarina, J.C.: Particle shape effects on packing density, stiffness, and strength: natural and crushed sands. *J Geotech Geoenviron Eng ASCE.* **132**(5), 591–602 (2006)
- Coop, M.R., Sorensen, K.K., Freitas, T.B., Georgoutsos, G.: Particle breakage during shearing of carbonate sand. *Geotechnique.* **54**(3), 157–163 (2004)

- Doumi, K., Cherif Taiba, A., Mahmoudi, Y., Belkhatir, M., Schanz, T. (2017). "Influence of gradation parameters on compaction of sand-silt mixtures: a laboratory assessment" International Symposium on Construction Management and Civil Engineering (ISCMCE-2017) Skikda-Algeria
- Feng, S.-J., Shui, W.-H., Tan, K., Gao, L.-Y., He, L.-J.: Field evaluation of dynamic compaction on granular deposits. *J Perform Constr Facil.* **25**(3), 241–249 (2011). [https://doi.org/10.1061/\(asce\)cf.1943-5509.0000160](https://doi.org/10.1061/(asce)cf.1943-5509.0000160)
- Galaa, A., Salem, M., Ibrahim, M., Hussein, A.: Static and cyclic shear behaviour of saline dredged sand. *Int J Geotech Eng.* 1–12 (2018). <https://doi.org/10.1080/19386362.2018.1550135>
- Gomez, A., Powers, R.F., Singer, M.J., Howarth, W.R.: Soil compaction effects on growth of young ponderosa pine following litter removal in California's Sierra Nevada. *Soil Sci Soc Am J.* **66**, 1334–1343 (2002)
- Gu, Q., Lee, F.H.: Ground response to dynamic compaction of dry sand. *Geotechnique.* **52**, 481–493 (2002)
- Janalizadeh, C., Ghalandarzadeh, A., Esmaeili, M.: Experimental study of the grading characteristic effect on liquefaction resistance of various graded sands and gravelly sands. *Arab Geosci.* (2013). <https://doi.org/10.1007/s12517-013-0886-5>
- Keramatikerman, M., Chegenizadeh, A., Nikraz, H.: Effect of fly ash on post cyclic behavior of sand. *J Earthq Eng.* (2018) ISSN: 1363-2469 (Print) 1559-808X
- Keramatikerman, M., Chegenizadeh, A., Nikraz, H., Sabbar, A.S.: Experimental study on effect of fly ash on liquefaction resistance of sand (2017). <https://doi.org/10.1016/j.soildyn.2016.11.012>
- Kim, D., Nam, B.H., Youn, H.: Effect of clay content on the shear strength of clay–sand mixtures. *Int J Geo-Eng.* **9**(1), (2018). <https://doi.org/10.1186/s40703-018-0087-x>
- Kolay, P.K., Puri, V.K., Lama Tamang, R., Regmi, G., Kumar, S.: Effects of fly ash on liquefaction characteristics of Ottawa sand. *Int J Geosynth Ground Eng.* (2019). <https://doi.org/10.1007/s40891-019-0158-x>
- Latifi, N., Horpibulsuk, S., Meehan, C.L., Abd Majid, M.Z., Tahir, M.M., Mohamad, E.T.: Improvement of problematic soils with biopolymer: an environmentally friendly soil stabilizer. *J Mater Civ Eng.* **29**(2), 04016204 (2017). [https://doi.org/10.1061/\(asce\)mt.1943-5533.0001706](https://doi.org/10.1061/(asce)mt.1943-5533.0001706)
- Liu, J., Wang, Y., Kanungo, D.P., Wei, J., Bai, Y., Li, D., Lu, Y.: Study on the brittleness characteristics of sand reinforced with polypropylene fiber and polyurethane organic polymer. *Fibers Polym.* **20**(3), 620–632 (2019). <https://doi.org/10.1007/s12221-019-8779-1>
- Mahmoudi, Y., Cherif Taiba, A., Belkhatir, M., Schanz, T.: Experimental investigation on undrained shear behavior of overconsolidated sand-silt mixtures: effect of sample reconstitution. *Geotech Test J.* **39**, 20140183 (2016a). <https://doi.org/10.1520/GTJ20140183>
- Mahmoudi, Y., Cherif Taiba, A., Belkhatir, M., Arab, A., Schanz, T.: Laboratory study on undrained shear behaviour of overconsolidated sand–silt mixtures: effect of the fines content and stress state. *Int J Geotech Eng.* **12**, 118–132 (2016b). <https://doi.org/10.1080/19386362.2016.1252140>
- Mahmoudi, Y., Cherif Taiba, A., Hazout, L., Wiebke, B.B.: Influence of soil fabrics and stress state on the undrained instability of overconsolidated binary granular assemblies. *Stud Geotech Mech.* **40**(2), 96–116 (2018). <https://doi.org/10.2478/sgem-2018-0011>
- Mahmoudi, Y., Cherif Taiba, A., Hazout, L., Belkhatir, M.: Experimental evidence into the impact of sample reconstitution on the pore water pressure generation of overconsolidated silty sand soils. *J GeoEng.* (2019). [https://doi.org/10.6310/jog.201912_14\(4\).3](https://doi.org/10.6310/jog.201912_14(4).3)
- Mahmoudi, Y., Cherif Taiba, A., Hazout, L., Belkhatir, M., Baille, W.: Packing density and overconsolidation ratio effects on the mechanical response of granular soils. *Geotech Geol Eng J.* **38**, 723–742 (2020). <https://doi.org/10.1007/s10706-019-01061-2>
- Meyerhof, G.G.: Safety factors in soil mechanics. *Can Geotech J.* **7**(4), 349–355 (1970). <https://doi.org/10.1139/t70-047>
- Nawagamuwa, N. Wijesooriya (2018), "Use of fly ash to improve soil properties of drinking water treatment sludge". *Int J Geoeng.* **V 9** (3), pp. 1–8
- NF P94-093: Sols Reconnaissance et essais-Détermination des références de compactage d'un matériau – Essai Proctor normal- Essai Proctor modifié. AFNOR (1999)
- Ören, A.H.: Estimating compaction parameters of clayey soils from sediment volume test. *Appl Clay Sci.* **101**, 68–72 (2014)
- Phanikumar, B.R., Nagaraju, T.V.: Effect of fly ash and rice husk ash on index and engineering properties of expansive clay. *Geotech Geol Eng.* (2018). <https://doi.org/10.1007/s10706-018-0544-5>
- Sabbar, A.S., Chegenizadeh, A., Nikraz, H.: Static liquefaction of very loose sand-slag-bentonite mixtures. *Soils Found.* **57**(3), 341–356 (2017). <https://doi.org/10.1016/j.sandf.2017.05.003>

- Saeid, A., Amin, C., Hamid, N.: Laboratory investigation on the compaction properties of lime and fly ash composite. In: International Conference on Civil and Architectural Applications (ICCAA'2012), (December 18–19, 2012), Thailand, pp. 79–83 (2012)
- Sanchez, F.G., Scott, D.A., Ludovici, K.H.: Negligible effects of severe organic matter removal and soil compaction on loblolly pine growth over 10 years. *For Ecol Manag.* **227**, 145–154 (2006)
- Wang, J.-J., Zhu, J.-G., Chiu, C.F., Chai, H.-J.: Experimental study on fracture behavior of a silty clay. *Geotech Test J.* **30**(4), 303–311 (2007)
- Wang, J.-J., Zhang, H.-P., Zhang, L., Liang, Y.: Experimental study on heterogeneous slope responses to drawdown. *Eng Geol.* **147–148**, 52–56 (2012)
- Wang, J.-J., Zhang, H.-P., Tang, S.-C., Liang, Y.: Effects of particle size distribution on shear strength of accumulation soil. *J Geotech Geoenviron Eng ASCE.* **139**(11), 1994–1997 (2013)
- Wei, L.M., Yang, J.: On the role of grain shape in static liquefaction of sand-fines mixtures. *Géotechnique.* **64**(9), 740–750 (2014)
- Xiao, Y., Long, L., Matthew Evans, T., Zhou, H., Liu, H., Stuedlein, A.W.: Effect of particle shape on stress-dilatancy responses of medium-dense sands. *J Geotech Geoenviron Eng.* **145**, 04018105 (2019). [https://doi.org/10.1061/\(ASCE\)GT.19435606.0001994](https://doi.org/10.1061/(ASCE)GT.19435606.0001994)
- Yilmaz, Y., Mollamahmutoglu, M., Ozaydin, V., Kayabali: Experimental investigation of effect of grading characteristics on the liquefaction resistance of various graded sands. *Eng Geol.* **J100**, 91–100 (2008)

Publisher's Note Springer Nature remains neutral with regard to jurisdictional claims in published maps and institutional affiliations.

Affiliations

Hamou Azaiez^{1,2} · Abdellah Cherif Taiba² · Youcef Mahmoudi² · Mostefa Belkhatir^{2,3}

¹ Laboratory of Structures, Geotechnics and Risks, University of Chlef, Chlef, Algeria

² Laboratory of Material Sciences & Environment, University of Chlef, Chlef, Algeria

³ Laboratory of Soil Mechanics, Foundation Engineering & Environmental Geotechnics, Bochum Ruhr University, Bochum, Germany